Available online at www.sciencedirect.com
SCIENCE DIRECT
Journal of Power Sources 143 (2005) 212–218
JOURNAL OF POWER SOURCES
www.elsevier.com/locate/jpowsour

Microstructure and electrochemical performance of $LiNi_{0.6}Co_{0.4-x}Mn_xO_2$ cathode materials

P.Y. Liao[a], J.G. Duh[a,*], S.R. Sheen[b]

[a] *Department of Materials Science and Engineering, National Tsing Hua University, Hsinchu, Taiwan*
[b] *Research Center for Applied Science, Academia Sinica, Nankang, Taipei, Taiwan*

Received 31 August 2004; accepted 5 December 2004
Available online 25 January 2005

Abstract

$LiNi_{0.6}Co_{0.4-x}Mn_xO_2$ ($0.15 \leqq x \leqq 0.25$) cathode materials for lithium-ion batteries are synthesized by calcining a mixture of $Ni_{0.6}Co_{0.4-x}Mn_x(OH)_2$ and Li_2CO_3 at 890–950 °C for 15 h in a flowing oxygen atmosphere. The $Ni_{0.6}Co_{0.4-x}Mn_x(OH)_2$ precursor is obtained by a chemical co-precipitation method at pH = 11. Thermal analysis of the precursor for $LiNi_{0.6}Co_{0.4-x}Mn_xO_2$ ($0.15 \leqq x \leqq 0.25$) shows that the weight loss is about 30% until the temperature reaches 750 °C. The X-ray diffraction patterns indicate the pure, layered, hexagonal structure of $LiNi_{0.6}Co_{0.4-x}Mn_xO_2$. Scanning electron micrographs reveal that the morphology of the samples is characterized by larger agglomerates (5–15 μm) of rather small layered particles (around 100 nm). The particle size tends to decrease with increasing Mn content. The electrochemical behaviour of $LiNi_{0.6}Co_{0.4-x}Mn_xO_2$ powder is examined by using test cells cycled within the voltage range 3–4.3 V at the 0.1 C rate for the first cycle and then at the 0.2 C rate. $LiNi_{0.6}Co_{0.4-x}Mn_xO_2$ ($0.15 \leqq x \leqq 0.25$) cathode materials exhibit good initial discharge capacity (165–180 mAh g^{-1}) and a capacity retention of above 95% after 20 cycles. It is demonstrated that $LiNi_xCo_yMn_{1-x-y}O_2$ electrodes are promising candidates for application as cathodes in lithium-ion batteries.
© 2004 Elsevier B.V. All rights reserved.

Keywords: Li-ion battery; Cathode material; Co-precipitation method; Cobalt doping; Lithium nickel oxide; Discharge capacity

1. Introduction

Lithium-ion batteries have played an important role in portable electronic devices during the past decade. Transition metal oxides such as $LiMn_2O_4$, $LiCoO_2$ and $LiNiO_2$ have been investigated extensively as cathode materials for such batteries [1–4]. Although $LiMn_2O_4$ is cost-effective, its capacity retention during cycling is poor [5]. $LiCoO_2$ is the most widely used cathode material because of its reasonable capacity (140–160 mAh g^{-1}) and high safety performance. Due to the high cost and toxicity of $LiCoO_2$, however, alternatives have been investigated. $LiNiO_2$ is the most attractive candidate by virtue of its lower cost and higher discharge capacity. Nevertheless, stoichiometric $LiNiO_2$ is difficult to synthesize because high-temperature treatment of $LiNiO_2$ leads to decomposition to $Li_{1-x}Ni_{1+x}O_2$, which has partial cation mixing between Li and Ni sites [6]. During cycling, lithium occupies nickel sites to cause structural instability and capacity deterioration [7]. Thus, to improve the properties of $LiNiO_2$, it is necessary to substitute Ni partially with other transition elements. Cobalt substitution can form a homogenous solid-solution over a large range of dopant content in $LiNi_{1-x}Co_xO_2$, since cobalt and nickel have similar properties.

In $LiNi_{1-x}Co_xO_2$ material, cobalt substitution can decrease cation mixing and stabilize the layer structure [7–9]. On the other hand, the introduction of expensive Co increases the fabrication cost. Recently, there have been reports [10–12] of adding a second element, Mn, to form multiple-ion doped lithium nickel oxides of lower cost. Moreover, layered $LiNi_{1-x-y}Co_xMn_yO_2$ material has been shown to be

* Corresponding author. Tel.: +886 3 5712686; fax: +886 3 5712686.
E-mail address: jgd@mx.nthu.edu.tw (J.G. Duh).

0378-7753/$ – see front matter © 2004 Elsevier B.V. All rights reserved.
doi:10.1016/j.jpowsour.2004.12.001

a most promising alternative material for $LiCoO_2$ because of its excellent electrochemical and safety characteristics. Li et al. [13] reported that the synthesis method has an effect on both the morphology and the electrochemical performance of $LiNi_{1/3}Mn_{1/3}Co_{1/3}O_2$ cathode materials [13]. The first discharge capacity of $LiNi_{1-x-y}Co_xMn_yO_2$ materials synthesized by a solid-state method [10] or sol–gel method [12] was about 150–165 mAh g^{-1} in the voltage range 3–4.3 V.

In this study, $LiNi_{0.6}Co_{0.4-x}Mn_xO_2$ cathode material is synthesized by the mixing hydroxide method that consists of two steps: (i) co-precipitation of transition metal salts in basic solution to form metal hydroxides with homogeneous cation distribution [14] and (ii) mixing of the hydroxides with Li_2CO_3 powder and then heating to various temperatures. Correlations between the calcining temperature and the Mn content in $LiNi_{0.6}Co_{0.4-x}Mn_xO_2$ materials are examined. The effect of Mn content on the morphology of $LiNi_{0.6}Co_{0.4-x}Mn_xO_2$ is also investigated.

2. Experimental

$NiSO_4{\cdot}6H_2O$, $CoSO_4{\cdot}7H_2O$ and $MnSO_4$ were used as starting materials and were dissolved in distilled water in a molar ratio of Ni^{2+}:Co^{2+}:Mn^{2+} = 0.6:(0.4 − x):x (x ranged from 0.15 to 0.25). A 1.5 M aqueous solution of the transition metal sulfates was slowly dripped into a mixed solution of 3 M NH_4OH and 4 M NaOH at a constant rate. The molar ratio of metal ions and ammonium was fixed and the pH value was adjusted to 11 by the addition of NaOH solution. The temperature was controlled at 60 °C to accelerate the rate of the co-precipitation reaction. After reacting for 10 h, the precipitate was filtered and washed several times to ensure that the residual ions (Na^+, SO_4^{2-}, or others) were almost removed. The precipitation was then dried at 110 °C overnight, and the $Ni_{0.6}Co_{0.4-x}Mn_x(OH)_2$ precursor with a homogeneous distribution was obtained. $Ni_{0.6}Co_{0.4-x}Mn_x(OH)_2$ and Li_2CO_3 were thoroughly mixed in ethanol using a mortar and pestle. These mixtures were heated to 890–950 °C for 15 h at a heating rate of 2 °C per min in a flowing oxygen atmosphere. The $LiNi_{0.6}Co_{0.4-x}Mn_xO_2$ cathode powder was formed and finally ground to pass through a 37-μm sieve.

Thermogravimetry/differential thermal analysis (Model-Pyris Diamond TG/DTA, Perkin-Elmer, USA) was employed to determine the appropriate calcining temperature. The phase composition and crystal structure of the heat-treated powder were analyzed by means of an X-ray diffractometer (XRD-6000, Shimadzu, Japan) that was operated at 30 kV and 20 mA from 15 to 80° at the wavelength of Cu Kα (λ = 1.5406 Å). The particle-size distribution of the $Ni_{0.6}Co_{0.4-x}Mn_x(OH)_2$ and $LiNi_{0.6}Co_{0.4-x}Mn_xO_2$ (x = 0.15 and 0.2) powders was examined by laser scattering (Horiba, LA 300, Japan). The particle morphology was observed by means of a field emission scanning electron microscope (FE-SEM, JSM-6500F, JEOL, Japan) at an accelerating voltage of 15 kV.

The electrochemical behaviour of $LiNi_{0.6}Co_{0.4-x}Mn_xO_2$ powder was examined in two-electrode test cells that consisted of a cathode, a metallic lithium anode, a polypropylene separator, and an electrolyte of 1 M $LiPF_6$ in a 1:1 (volume ratio) mixture of ethylene carbonate (EC) and diethyl carbonate (DEC). The electrode (cathode) was made by mixing a slurry of 91 wt.% $LiNi_{0.6}Co_{0.4-x}Mn_xO_2$ powder with 6 wt.% super P carbon black, and 3 wt.% polyvinylidene fluoride binder (PVDF) in *N*-methyl pyrrolidinone (NMP). The slurry was then coated on aluminum foil and dried at 130 °C for more than 3 h. Using these electrodes, 2016 type coin-cells were assembled in an argon glove-box where both moisture and oxygen content were <2 ppm. The cells were cycled over the voltage range 3–4.3 V at the 0.1 C rate for the first cycle and then at the 0.2 C rate.

3. Results and discussion

3.1. Thermal analysis

The TG/DTA profiles for the precursor $LiNi_{0.6}Co_{0.4-x}Mn_xO_2$ materials for various values of x that range from 0.15 to 0.25 are presented in Fig. 1(a)–(c). There is a little change in the profiles as the Mn content is increased. The weight loss from room temperature to 150 °C can be assigned to the loss of water adsorbed on the surfaces and some intercalated water molecules that are bonded to hydroxyl groups [15]. The endothermic peak around 200–250 °C in an oxygen atmosphere may be due to the decomposition of $M(OH)_2$ ($M = Ni_{0.6}Co_{0.4-x}Mn_x$) to spinel phase M_3O_4 [15]. Although Li_2CO_3 is stable in air up to 750 °C and the melting point is 723 °C, some studies have indicated [16,17] that Li_2CO_3 already reacts below 300 °C. The exothermic peaks around 300–400 °C result from a decomposition reaction of Li_2CO_3 to Li_2O and subsequent diffusion of lithium ions into M_3O_4 crystals to form M_3O_4 with interstitial Li_2O [17]. The hexagonal phase $LiNi_{0.6}Co_{0.4-x}Mn_xO_2$ materials form at higher temperatures. The weight loss is almost zero after 800 °C, which indicates that $LiNi_{0.6}Co_{0.4-x}Mn_xO_2$ completely forms at this temperature.

3.2. Phase identification

The X-ray diffraction patterns of $LiNi_{0.6}Co_{0.4-x}Mn_xO_2$ with x = 0.15, 0.2 or 0.25 calcined in various temperatures are given in Fig. 2 with Miller indexes indicated. All of the peaks can be indexed based on the hexagonal α-$NaFeO_2$ structure. In this structure, Li atoms are at the 3a sites, transition metal atoms Ni, Co, and Mn are randomly distributed at the 3b sites, and O atoms are at the 6c sites. No impurity phase is observed in the XRD patterns of $LiNi_{0.6}Co_{0.4-x}Mn_xO_2$ synthesized by the mixed hydroxide method. In these patterns, the intensity ratios of the (0 0 3) and (1 0 4) lines are larger than 1.1 and splitting of the (0 0 6, 0 1 2) and (0 1 8, 1 1 0) lines is clearly observed. This implies that less cation mixing is present in $LiNi_{0.6}Co_{0.4-x}Mn_xO_2$ (x = 0.15, 0.2, 0.25) [18].

Table 1
Lattice parameters of $LiNi_{0.6}Co_{0.25}Mn_{0.15}O_2$ calcined at temperatures between 890 and 920 °C

Temperature (°C)	a (Å)	c (Å)	c:a ratio	Unit cell volume (Å^3)	I_{003}/I_{104} ratio
890	2.8622	14.1902	4.9577	100.68	1.26
900	2.8630	14.1894	4.9561	100.73	1.32
910	2.8639	14.1991	4.9580	100.86	1.22
920	2.8642	14.2075	4.9603	100.94	1.53

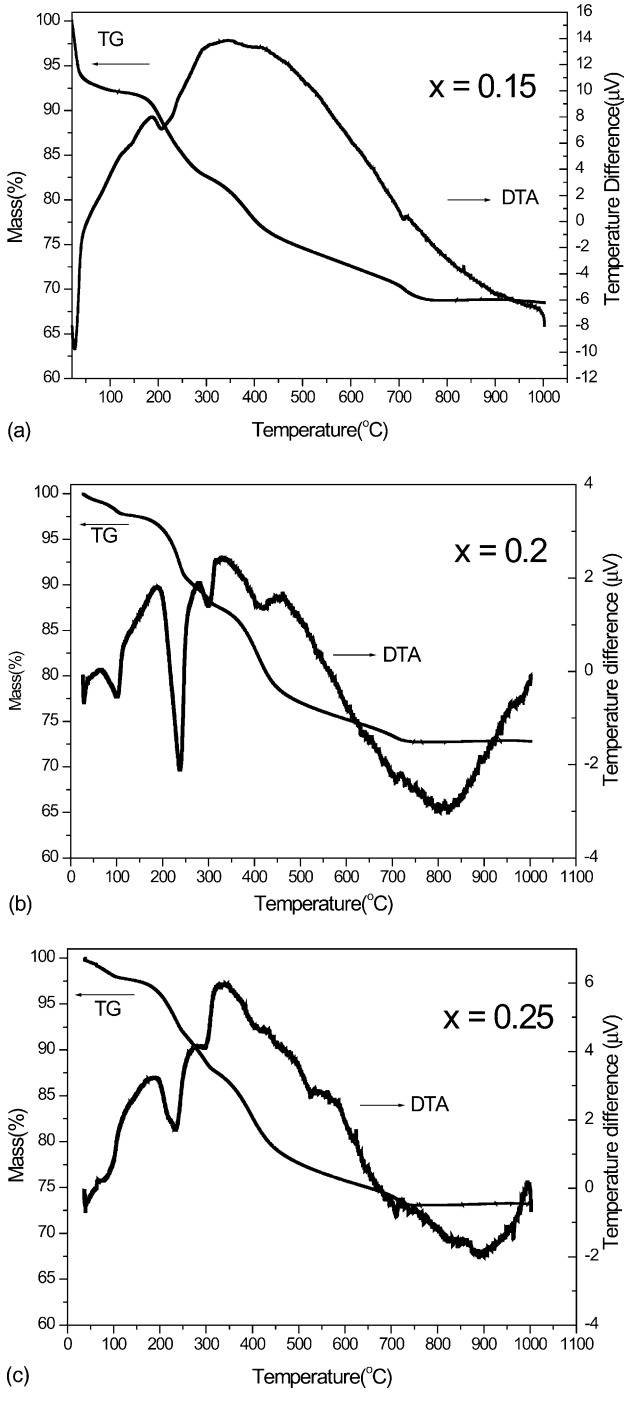

Fig. 1. TG/DTA profiles for $LiNi_{0.6}Co_{0.4-x}Mn_xO_2$ ($x = 0.15$, 0.2, 0.25) precursor heat-treated from room temperature to 1000 °C at 2 °C per min in air.

The lattice parameters, a and c, calculated by the least-squares method with 10 diffraction lines and the I_{003}/I_{104} ratio of a $LiNi_{0.6}Co_{0.4-x}Mn_xO_2$ sample with $x = 0.15$ calcined at 890–920 °C are listed in Table 1. With increasing heating temperature, the a- and c-axes expand, and thus the hexagonal unit-cell volume, i.e., $(3)^{1/2}a^2c/2$, increases from 100.677 Å^3 at 890 °C to 100.94 Å^3 at 920 °C. Choi et al. [18] reported that if partial cation mixing occurs, it will cause a decrease in the c:a ratio [18]. The lowest c:a ratio at 900 °C suggests the formation of a mixture of the cubic and hexagonal structures.

3.3. Particle size and morphology

Micrographs of the $Ni_{0.6}Co_{0.25}Mn_{0.15}(OH)_2$ precursor synthesized by the co-precipitation method after 10 h are presented in Fig. 3. The samples are composed of agglomerates (5–15 μm) of very small layered particles (about 100 nm), as shown in Fig. 3(b). There are two growth stages during the formation of the hydroxide precipitation. First, in violent stirring solution, cations and hydroxyl groups react to form primary precipitates of $M(OH)_2$ ($M = Ni_{0.6}Co_{0.4-x}Mn_x$). As the reaction time is increased, the small particles slowly agglomerate to form secondary spherical particles. The morphologies of primary particles on the surfaces of $LiNi_{0.6}Co_{0.25}Mn_{0.15}O_2$ powders calcined at temperatures between 890 and 910 °C for 15 h are presented in Fig. 4. There is an evident distinction in morphology between hydroxides and oxides. $LiNi_{0.6}Co_{0.25}Mn_{0.15}O_2$ oxides do not exhibit an apparent layered habit, as compared with $Ni_{0.6}Co_{0.4-x}Mn_x(OH)_2$ materials. After heat treatment, rock-shaped grains form on the surface. As the calcined temperature is raised, the grain size increases and the edges of the grains become shaper.

The average size of primary particles are shown in Fig. 5 as a function of temperature with different Mn contents calcined at various temperatures. With increasing Mn content, the primary particle size decreases at a specific temperature. For example, for $LiNi_{0.6}Co_{0.4-x}Mn_xO_2$ calcined at 910 °C, the average particle size is 0.8 μm at $x = 0.15$, while it is 0.54 μm at $x = 0.2$ and 0.53 μm at $x = 0.25$. Thus, the particle size is influenced by the Mn content. The particle size tends to decrease with increasing Mn content.

3.4. Electrochemical properties

The electrochemical behaviour of $LiNi_{0.6}Co_{0.4-x}Mn_xO_2$ calcined at various temperatures has also been investigated.

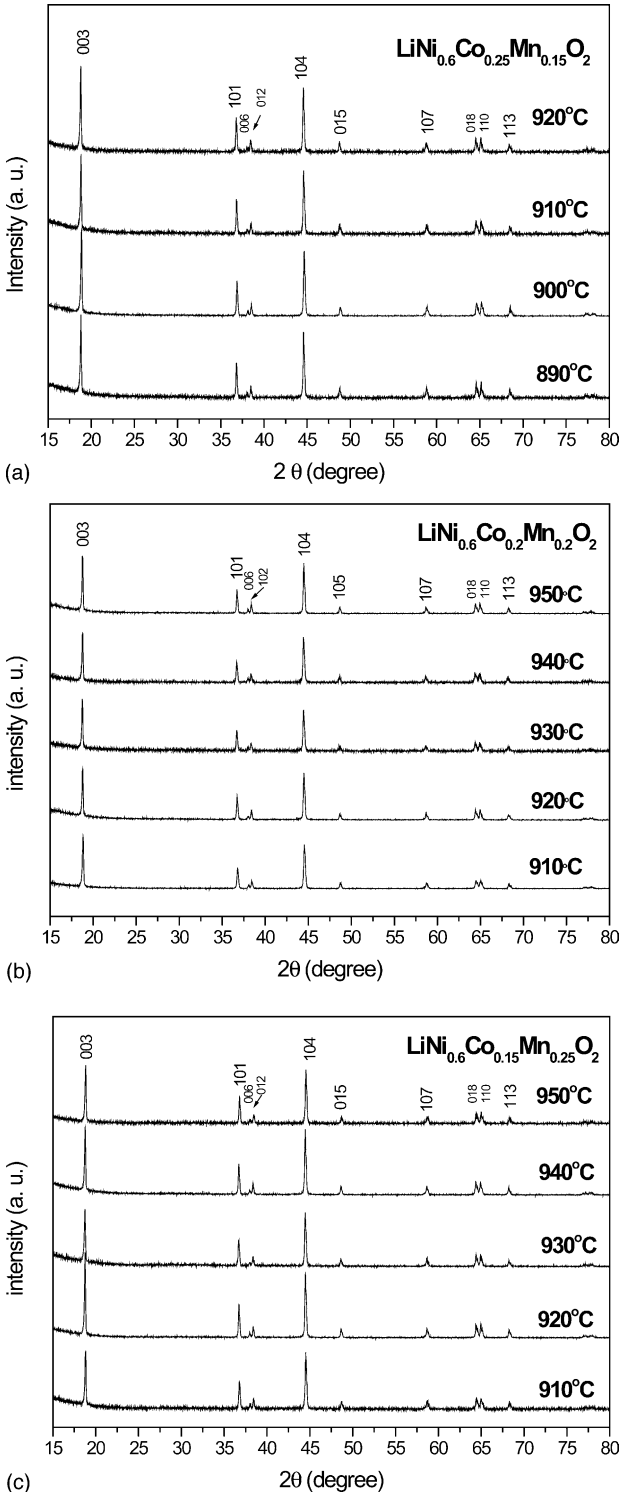

Fig. 2. X-ray diffraction patterns for $LiNi_{0.6}Co_{0.4-x}Mn_xO_2$ (a) $x = 0.15$, (b) $x = 0.2$ and (c) $x = 0.25$ calcined at various temperatures in oxygen atmosphere.

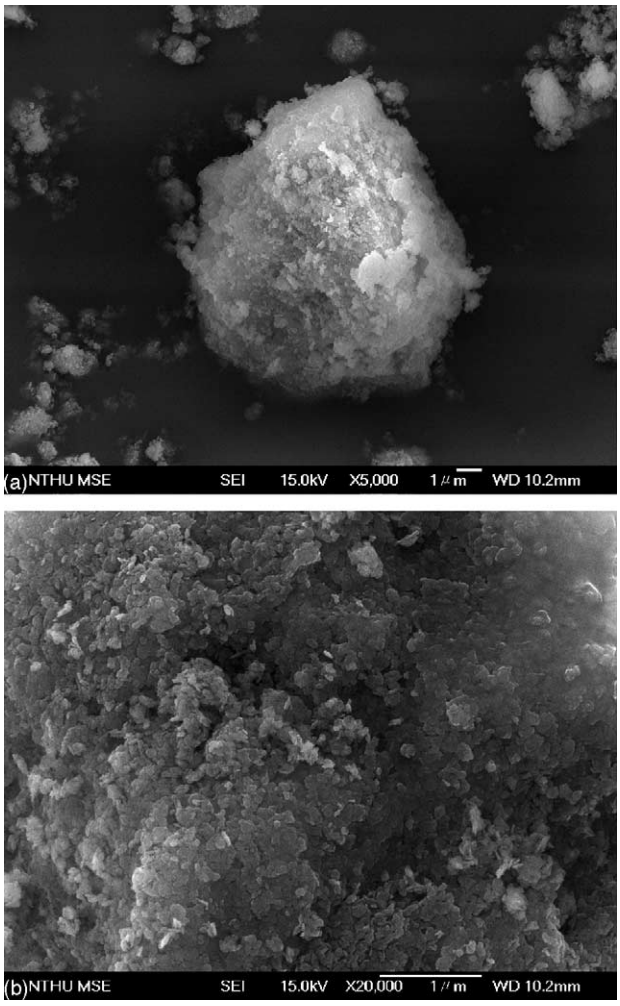

Fig. 3. Scanning micrographs of (a) $Ni_{0.6}Co_{0.25}Mn_{0.15}(OH)_2$ and (b) the surface morphology of $Ni_{0.6}Co_{0.25}Mn_{0.15}(OH)_2$ powder.

The first charge–discharge profiles of $LiNi_{0.6}Co_{0.4-x}Mn_xO_2$ with $x = 0.15$ calcined at temperatures between 890 and 920 °C and cycled between 3 and 4.3 V at the 0.1 C rate are given in Fig. 6. The curves are quite smooth without any plateaux. This implies that there is no transformation from a cubic to a spinel phase during charging and discharging [19]. The first irreversible capacities, i.e., the difference between the first charge and discharge capacity, are about 20 mAh g^{-1} for $LiNi_{0.6}Co_{0.25}Mn_{0.15}O_2$. This is attributed to the formation of a passivation film on the surface of the electrode [20].

The discharge capacity as a function of cycle number for $LiNi_{0.6}Co_{0.25}Mn_{0.15}O_2$ samples calcined between 890 and 920 °C is given in Fig. 7. Cycling tests were operated within the voltage range 3–4.3 V at the 0.1 C rate for the first cycle and then at the 0.2 C rate. The initial discharge capacities are similar (about 175–178 mAh g^{-1}). The sample calcined at 900 °C exhibits the best electrochemical performance; it has a discharge capacity of 178.4 and 175 mAh g^{-1} on the first and 20th cycles, respectively. When calcined at 890 and 910 °C, $LiNi_{0.6}Co_{0.25}Mn_{0.15}O_2$ exhibits excellent capacity retention—the efficiency is about 95 and 96%, respectively, after 20 cycles. By contrast, the discharge capacity of $LiNi_{0.6}Co_{0.25}Mn_{0.15}O_2$ calcined at 920 °C retains only 91.2% of its original value after 20 cycles.

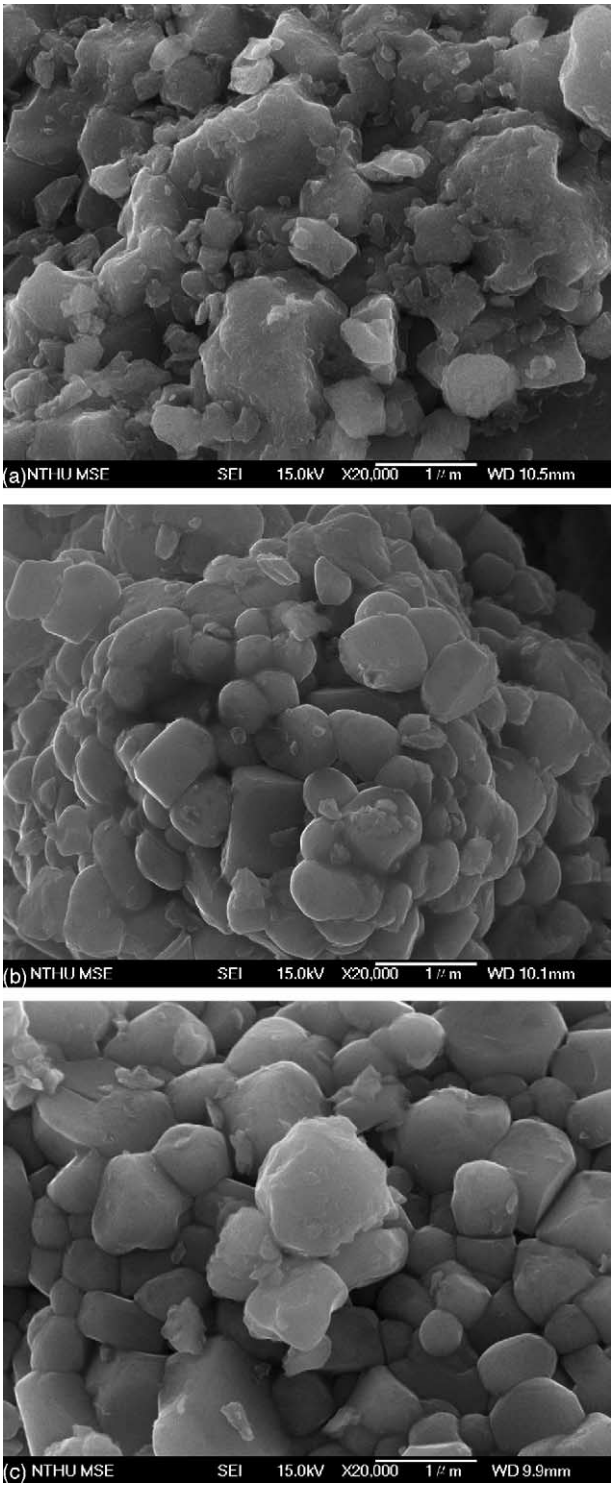

Fig. 4. . FESEM images of $LiNi_{0.6}Co_{0.25}Mn_{0.15}O_2$ calcined at (a) 890, (b) 900 and (c) 910 °C for 15 h.

The electrochemical properties of $LiNi_{0.6}Co_{0.4-x}Mn_xO_2$ for $x = 0.15$, 0.2 and 0.25 are summarized in Table 2. When both high initial capacity and capacity retention are considered in $LiNi_{0.6}Co_{0.2}Mn_{0.2}O_2$, the sample calcined at 940 °C shows the best behaviour. The initial discharge capacity of

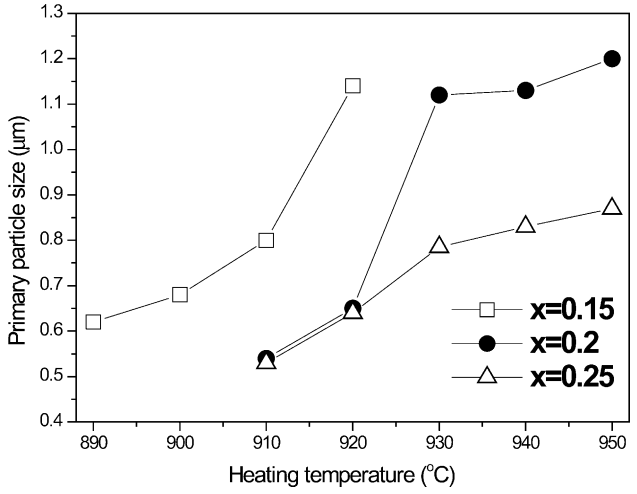

Fig. 5. Average particle size of primary powders as function of temperature for $LiNi_{0.6}Co_{0.4-x}Mn_xO_2$ materials ($x = 0.15$, 0.2, 0.25).

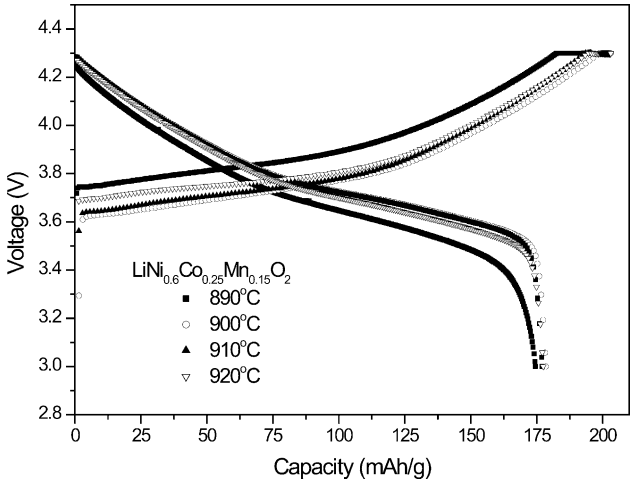

Fig. 6. First charge–discharge profile for $LiNi_{0.6}Co_{0.4-x}Mn_xO_2$ for $x = 0.15$ calcined at (a) 890, (b) 900, (c) 910 and (d) 920 °C between 3 and 4.3 V at 0.1 C rate.

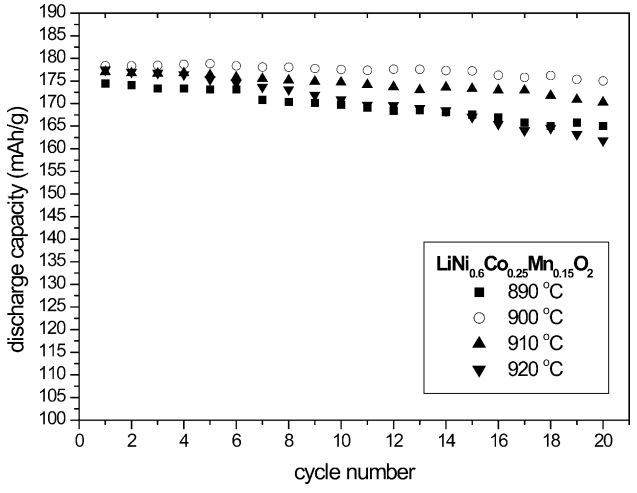

Fig. 7. Specific discharge capacities of $LiNi_{0.6}Co_{0.25}Mn_{0.15}O_2$ calcined at temperatures between 890 and 920 °C for 15 h cycled at 0.2 C rate between 3 and 4.3 V at room temperature.

Table 2
Electrochemical properties of $LiNi_{0.6}Co_{0.4-x}Mn_xO_2$ ($x = 0.15, 0.2, 0.25$)

X	Calcination temperature (°C)	1st discharge capacity (mAh g^{-1})	20th discharge capacity (mAh g^{-1})	Capacity retention after 20 cycles (%)
0.15	890	174.5	165.0	94.6
	900	178.4	175.0	98.1
	910	177.0	170.3	96.2
	920	177.4	161.8	91.2
0.2	910	166.6	161.6	97.0
	920	170.7	163.6	95.8
	930	171.3	165.8	96.8
	940	175.6	169.7	96.6
	950	168.6	159.6	94.6
0.25	910	173.7	158.9	91.5
	920	171.3	147.3	86.0
	930	170.4	160.3	94.1
	940	168.4	158.3	94.0
	950	167.2	163.3	97.7

the $LiNi_{0.6}Co_{0.15}Mn_{0.25}O_2$ material decreases with calcining temperature. On the other hand, raising the calcining temperature has a positive effect on capacity retention. The sample calcined at 950 °C displays the best electrochemical properties due to its high capacity retention. It should be noted that in determining the optimum particle size of cathode materials for electrode fabrication, attention should be paid to the carbon black used in mixing the slurry [21]. In other words, the particle size of the cathode material is not the sole determinant of the electrochemical properties observed in this study.

The data presented in Table 2 show that most beneficial calcining temperature of $LiNi_{0.6}Co_{0.4-x}Mn_xO_2$ samples increases with the Mn content. Overall, $LiNi_{0.6}Co_{0.4-x}Mn_xO_2$ materials ($x = 0.15$, 0.2, 0.25) derived by the mixing hydroxide method exhibit good electrochemical behaviour.

4. Conclusions

Layered, hexagonal structure $LiNi_{0.6}Co_{0.4-x}Mn_xO_2$ ($x = 0.15$, 0.2, 0.25) materials have been successfully synthesized by the mixing hydroxide method. As the heating temperature increases, primary rock-shaped grains form on the surface of the materials. When the Mn content is increased, the primary particle size of $LiNi_{0.6}Co_{0.4-x}Mn_xO_2$ prepared at the same calcining temperature tends to decrease.

The $LiNi_{0.6}Co_{0.4-x}Mn_xO_2$ ($x = 0.15$, 0.2, 0.25) materials exhibit excellent electrochemical properties. With increase in Mn content, the calcining temperature should be increased to enhance the electrochemical properties. In this study, $LiNi_{0.6}Co_{0.25}Mn_{0.15}O_2$ calcined at 900 °C exhibits the best electrochemical characteristics, for which the initial discharge capacity reaches 178.4 mAh g^{-1} and the capacity retention is 98.1% after 20 cycles. It is concluded that $LiNi_{1-x-y}Co_yMn_xO_2$ compounds are promising low-cost cathode materials for lithium-ion batteries.

Acknowledgments

The first two authors are grateful to the Coremax Taiwan Corporation, Taiwan, for financial support and to the General Manager, Mr. J. Ho, for his endorsement of the project. Partial support from National Science Council, Taiwan, under the contract No. NSC-92-2216-E007-037 is also acknowledged.

References

[1] J.R. Dahn, U. von Sacken, C.A. Michal, Solid State Ionics 44 (1990) 87–97.
[2] T. Ohzuku, A. Ueda, M. Nagayama, Y. Iwakoshi, H. Komori, Electrochim. Acta 38 (1993) 1159–1167.
[3] K. Mizushima, P.C. Jones, P.J. Wiseman, J.B. Goodenough, Mater. Res. Bull. 15 (1980) 783–789.
[4] M.M. Thackeray, W.I.F. David, P.G. Bruce, J.B. Goodenough, Mater. Res. Bull. 18 (1983) 461–472.
[5] H.W. Chan, J.G. Duh, S.R. Sheen, J. Power Sources 115 (2003) 110–118.
[6] J. Morales, C. Perez-Vicente, J.L. Tirado, Mater. Res. Bull. 25 (1990) 623–630.
[7] C. Delmas, M. Ménétrier, L. Croguennec, I. Saadoune, A. Rougier, C. Pouillerie, G. Prado, M. Grüne, L. Fournès, Electrochim. Acta 45 (1999) 243–253.
[8] M. Okada, K. Takahashi, T. Mouri, J. Power Sources 68 (1997) 545–548.
[9] C.C. Chang, N. Scarr, P.N. Kumta, Solid State Ionics 112 (1998) 329–344.
[10] M. Yoshio, H. Noguchi, J. Itoh, M. Okada, T. Mouri, J. Power Sources 90 (2000) 176–181.
[11] Y. Sun, C. Ouyang, Z. Wang, X. Huang, L. Chen, J. Electrochem. Soc. 161 (2004) 504–508.
[12] B.J. Hwang, Y.W. Tsai, C.H. Chen, R. Santhanam, J. Mater. Chem. 13 (2003) 1962–1968.
[13] D.C. Li, T. Muta, L.Q. Zhang, M. Yoshio, H. Noguchi, J. Power Sources 132 (2004) 150–155.

[14] C.C. Yang, Int. J. Hydrogen Energy 27 (2002) 1071–1081.
[15] S. Jouanneau, J.R. Dahn, Chem. Mater. 15 (2003) 495–499.
[16] D.R. Lide, CRC Handbook of Chemistry and Physics, 83rd ed. Chemical Rubber Company, Ohio, USA, 2002, Chapter 4, 66 pp.
[17] A. Lundblad, B. Bergman, Solid State Ionics 96 (1997) 173–181.
[18] Y.M. Choi, S.I. Pyun, S.I. Moon, Solid State Ionics 89 (1994) 43–52.
[19] A. Robert Armstrong, P.G. Bruce, Nature 381 (1996) 499–500.
[20] G.X. Wang, S. Bewlay, J. Yao, Y. Chen, Z.P. Guo, H.K. Liu, S.X. Dou, J. Power Sources 119–121 (2003) 189–194.
[21] P.Y. Liao, J.G. Duh, Key Eng. Mater. 280–283 (2005) 677–681.